Carbohydrate Polymers
Manuscript Draft

Manuscript Number: CARBPOL-D-15-02024

Title: Nanofiller for the mechanical reinforcement of maltodextrins orodispersible films

Article Type: Research Paper

Keywords: Orodispersible films; maltodextrins; nanofiller; mechanical reinforcement; tensile properties; casting solution.

Abstract: One of the most critical quality attributes of orodispersible films (ODFs) is related to the development of dosage forms with tensile properties suitable for the packaging and patient's handling. Aiming to individuate a strategy to reinforce the tensile properties, the current work reported the feasibility to improve the tensile strength of maltodextrins (MDX) based ODFs by adding an amorphous water insoluble nanofiller, namely polyvinylacetate (PVAc).
The possible interactions between components investigated by DSC and ATR-FTIR spectroscopy revealed that MDX and PVAc were immiscible; even if, the presence of plasticizers permitted the homogeneous dispersion of PVAc in the film until the 10% w/w strength was reached. As a consequence, PVAc nanoparticles resulted an effective reinforcing agent only at the concentrations of 3 and 5 % w/w. In this optimal range, the tensile strength increased of at least 1.5 fold and the elastic modulus increased of at least 4 times.

Highlights

- The tensile properties of maltodextrin orodispersible films were improved by loading polyvinyl acetate (PVAc) nanoparticles at the concentrations of 3 and 5 % w/w.
- Maltodextrin and PVAc are immiscible.
- The presence of plasticizers, namely glycerin and sorbitan monoleate, favored the homogenous dispersion of PVAc nanoparticles to the strength of 10% w/w.

Nanofiller for the mechanical reinforcement of maltodextrins orodispersible films

Ilaria FRANCESCHINI[1], Francesca SELMIN[1], Stefania PAGANI[2§], Paola MINGHETTI[1], Francesco CILURZO[1]*

Affiliations

[1] Department of Pharmaceutical Sciences – Università degli Studi di Milano - Via G. Colombo, 71 – 20133 Milan - Italy

[2] BOUTY S.p.A. - S.S. n°11, Padana Superiore km 160 - 20060 Cassina de' Pecchi (MI) - Italy

Email address: ilaria.franceschini@unimi.it (Ilaria Franceschini); francesca.selmin@unimi.it (Francesca Selmin); Stefania.Pagani@adarepharma.com (Stefania Pagani); paola.minghetti@unimi.it (Paola Minghetti); francesco.cilurzo@unimi.it (Francesco Cilurzo)

**To whom the correspondence should be sent:*

Prof. Francesco Cilurzo, PhD
Department of Pharmaceutical Sciences – Università degli Studi di Milano
Via Giuseppe Colombo, 71 – 20133 Milan (Italy)
Phone: +39 02 503 24635
Fax: + 39 02 503 24657
Email: francesco.cilurzo@unimi.it

§ Permanent address:

Adare Pharmaceuticals S.r.l. - Via Martin Luther King, 13 - 20060 Pessano con Bornago (MI) - Italy

Abstract

One of the most critical quality attributes of orodispersible films (ODFs) is related to the development of dosage forms with tensile properties suitable for the packaging and patient's handling. Aiming to individuate a strategy to reinforce the tensile properties, the current work reported the feasibility to improve the tensile strength of maltodextrins (MDX) based ODFs by adding an amorphous water insoluble nanofiller, namely polyvinylacetate (PVAc).

The possible interactions between components investigated by DSC and ATR-FTIR spectroscopy revealed that MDX and PVAc were immiscible; even if, the presence of plasticizers permitted the homogeneous dispersion of PVAc in the film until the 10% w/w strength was reached. As a consequence, PVAc nanoparticles resulted an effective reinforcing agent only at the concentrations of 3 and 5 % w/w. In this optimal range, the tensile strength increased of at least 1.5 fold and the elastic modulus increased of at least 4 times.

Keywords:

Orodispersible films; maltodextrins; nanofiller; mechanical reinforcement; tensile properties; casting solution.

1. Introduction

Orodispersible films (ODFs) are fast-dissolving dosage forms intended to deliver drugs both locally and systemically after administration in the oral cavity. ODFs have gained an increased interest in academic and industrial world because they have a huge clinical potential to legitimate expectations of special subpopulations, such as pediatric, elderly and dysphagic patients, who have difficulty in swallowing conventional tablets and capsules (Borges, Silva, Coelho, & Simões, 2015; Dixit & Puthli, 2009). ODFs made of maltodextrins (MDX) with a dextrose equivalent in the 6-12 range, have been successfully proposed due to suitable filmogenic properties, high water solubility and low cost (Cilurzo, Cupone, Minghetti, Selmin, & Montanari, 2008). From a technological point of view, ODFs are generally processed by casting an aqueous solution of MDX properly plasticized by hydrogen-bonding plasticizing agent (e.g., glycerol and natural aminoacids), the active compound of interest and some other functional ingredients (e.g., taste-masking agents and flavours) (Cilurzo et al., 2011; Selmin, Franceschini, Cupone, Minghetti, & Cilurzo, 2015). After solvent evaporation, the film is further processed, namely cut into a desirable size and shape and packed. The preparation of films for oromucosal drug delivery is challenging compared to other dosage forms. Indeed, depending on the physical-chemical characteristics of the ingredients loaded and their amount in the formulation, modifications of the mechanical properties can occur resulting in films too flexible or brittle to guarantee the integrity. As an example, the incorporation of an oily drug slightly increased plasticity acting as a plasticizer (Cilurzo et al., 2010). However, as also stated by European Pharmacopoeia (EDQM) the mechanical strength of ODFs is of paramount importance since they should resist handling without being damaged or broken. Currently, there is a growing tendency to develop polymeric film reinforced with nanoparticles to avoid this drawback. For instance, starch-based matrix materials loaded with nanosized fillers, e.g. clay minerals (Chen & Evans, 2005; De Carvalho, Curvelo, & Agnelli, 2001; Wilhelm, Sierakowski, Souza, & Wypych, 2003) or polymers (Le Bolay, Lamure, Gallego Leis, & Suhani, 2012; Le Bolay & Molina-Boisseau, 2014), exhibited drastic modification in their properties, such as improved tensile strength and elongation and decreased the vapour diffusion (Park, H. W., Lee, Park, C. Y., Cho, & Ha, 2003). Generally speaking, it was demonstrated that the extent of the reinforcement depends on such factors as (i) the elastic properties of its constitutive phases, (ii) the volume fraction of filler (iii) the morphology (i.e., shape, aspect ratio, and distribution of the filler into the polymeric matrix) and (iv) the interactions between fillers. However, the low interfacial compatibility between polymer and filler can result in the poor dispersion of nanofiller in the polymeric matrix. Consequently, the formation of nanoparticles agglomerates as a consequence of their high specific surface area or hydrogen bonding ability, may result in lower final properties (Petersson & Oksman, 2006). Homogeneous dispersion of nanoparticles can be achieved preparing nanocomposites in solution by solvent casting methods or by blending and compatibilization with components, which display complementary properties and can

contribute to improve the nanofiller dispersion through effective interaction at the interface (Fortunati, Puglia, Kenny, Haque, & Pracella, 2013).

In view of the above considerations, the current work reports a comprehensive investigation on the behavior of plasticized MDX based ODFs loaded with different amounts of an amorphous water insoluble nanofiller, namely Kollicoat® SR 30 D (PVAc). The tensile properties of the nanocomposite films were studied taking in account the possible interactions between the polymers at molecular level.

2. Materials and Methods

2.1. Materials

Maltodextrins having a DE equal to 6 (Glucidex® IT6, MDX) was obtained from Roquette Frères (F). Kollicoat® SR 30 D (PVAc) was kindly gifted by BASF (G). It is a 27 % w/w colloidal aqueous polymer dispersion of polyvinylacetate with a particle size of about 170 nm stabilized by sodium lauryl sulfate (0.3 % w/w) and povidone (2.7 % w/w) (Kolter, Dashevsky, Irfan, & Bodmeier, 2013). Sorbitan monooleate (Span® 80, S80) was purchased by Uniqema (UK) and glycerol (GLY) was obtained by Carlo Erba Reagenti (I). All materials were used without any further manipulation.

2.2. Preparation of binary mixtures

Aqueous feeds were prepared dissolving MDX and PVAc in the same ratio as in the placebo films as following: 99/1, 97/3, 95/5, 90/10 and 80/20 % w/w. Binary mixtures were prepared by using a spray-dryer (Formate 4 M8 – ProCepT, B). Process parameters were set as follows: standard nozzle inner diameter: 0.6 mm; air speed 0.30 m^3/min; air in temperature: 130 °C; dosing speed: 7 mL/min.

2.3. Differential scanning calorimetry

In order to characterize the thermal behavior of the binary mixture made of MDX and PVAc in comparison with the raw materials, DSC was performed by using a DSC 1 Star^e System (Mettler Toledo, CH). Samples of about 8 mg accurately weighted were sealed in pin holed aluminum pans and heated from 0 to 150 °C at the cooling and heating rate of 5 K/min. The DSC cell and RCS were purged with dry nitrogen at 80 and 120 mL/min, respectively. The glass transition temperature (T_g) was taken as the inflection point of the specific heat increment at the glass–rubber transition. Three samples were tested for each formulation and data expressed as their average ± standard deviation.

2.4. ATR-FTIR measurements

The absorption of the spray-dried binary blends were collected in the spectral range of 4000–650 cm^{-1} using a Spectrum^{TM}One spectrometer (PerkinElmer, I) equipped with an attenuated total reflectance (ATR)

accessory. The optical resolution of the spectrometer was 4 cm^{-1} and 256 spectra were summed prior to the analysis. A duplicate spectrum was collected for each sample after 4 min in order to check that the measurements were not affected by sorption of water vapor during the experiments. No measurable differences were observed between the two spectra (data not shown).

The absorption spectra were firstly smoothed using the Origin® 9.1 (OriginLab Corporation, USA) and the position of the maximum of the broad peaks was determined by analysis of the second derivative.

2.5. Film preparation

Films were prepared by the solvent casting technique as previously described (Cilurzo et al., 2008). Briefly, MDX were dissolved in water obtained from a Milli-Q® Integral 3 (Merck Millipore Corporation, G) filter system at 80 °C, according to the composition reported in **Table 1**. The dispersion was cooled down to 40 °C, all the other ingredients were added and stirred until homogeneity. After a rest period to remove bubbles, the dispersion was cast over a silicone release liner by a laboratory-coating unit Mathis LTE-S(M) (CH). Operative conditions: coating rate 1 m/min; drying temperature 60 °C; drying time between 15-20 min; air circulation speed 1,800 rpm. These conditions were set to obtain films having a thickness of about 100 µm.

Films were cut into suitable shape and size as required for testing, packed in individual air-tight seal packs immediately after preparation and stored at 25°C until use.

2.6. Film characterization

Thickness

Film thickness was measured by using a MI 1000 (ChemInstruments, USA). The accuracy of the instrument was 2.5 µm ± 0.5%. Before samples cutting, film was placed between the anvil and the presser foot of the micrometer. Film thickness was measured in ten different positions and the result was expressed as the mean value.

Moisture content

The moisture content (*MC*) was determined gravimetrically after keeping films samples of 6 cm^2 surface at the temperature of 130 °C over a 2 hour period. The results were expressed as the mean of three determination according to the following equation:

$$MC = \frac{W_0 - W_f}{W_0} \times 100$$

where W_0 and W_f are the initial and final weight, respectively.

Disintegration test

Disintegration test of films was carried out on 3x2 cm sample according to specifications of tablets and capsules reported in European Pharmacopoeia 7th Ed. 2013.

2.7. Tensile properties

Tensile testing was conducted using a texture analyzer AG/MC1 (Acquati, I), equipped with a 5 N load cell. The film was cut into 100×15.0 mm strips and equilibrated at 25 °C for 1 week. Tensile tests were performed according to ASTM International Test Method for Thin Plastic Sheeting (D 882-02). Each test strip was longitudinal by placed in the tensile grips on the texture analyzer. Initial grip separation was 40 mm and crosshead speed was 25 mm/min. The test was considered concluded at the film break. Tensile strength, elongation at break, elastic modulus and work were computed to evaluate the tensile properties of the films.

Tensile strength (TS) was calculated by dividing the maximum load by the original cross-sectional area of the specimen and it was expressed in force per unit area (MPa).

Percent elongation at break (E%) was calculated by dividing the extension at the moment of rupture of the specimen by the initial gage length of the specimen and multiplying by 100 according to the following equation:

$$E\% = \frac{L - L_0}{L_0} \times 100$$

where L_0 is the initial gage length of the specimen and L is the length at the moment of rupture.

Elastic modulus or *Young's modulus* (Y) was calculated as the slope of the linear portion of the stress– strain curve. The result was expressed in force per unit area (MPa).

Tensile energy to break (TEB) was defined by the area under the stress–strain curve. The value is in units of energy.

An average of five measurements was taken for each type of specimen.

3. Results and discussion

3.1. Characterization of nanocomposite films

Films loaded by PVAc in the composition range reported in **Table 1** were homogeneously opaque in appearance, while the film F0 appeared transparent. The residual moisture content was about 10 % (w/w) in all formulations. All films were handled, cut, and packed without failure. Nanocomposite films

disintegrated in less than 1 minutes evidencing that the addition of PVAc in different ratios did not affect the dissolution of MDX.

Table 1 – Effect of concentration of PVAc on tensile strength (TS), percentage elongation at break (E%), tensile energy to break (TEB) and elastic modulus (Y) in MDX nanocomposite films. The results are expressed as the mean of five measurements ± standard deviation.

Form. code	Composition (% w/w)				TS (MPa)	E% (%)	TEB (J)	Y (MPa)
	MDX	GLY	S80	PVAc				
F0	79.0	18.0	3.0	--	1.8±0.8	23.5±4.8	0.010±0.003	4.2±2.9
F1	78.2	17.8	3.0	1.0	1.9±0.4	26.5±3.9	0.007±0.001	8.9±2.5
F3	76.5	17.5	3.0	3.0	7.3±1.1	34.4±8.0	0.026±0.007	27.2±3.5
F5	74.9	17.1	3.0	5.0	3.7±0.7	58.8±12.5	0.027±0.009	11.1±3.6
F10	70.8	16.2	3.0	10.0	2.8±0.4	39.0±5.7	0.012±0.002	9.3±1.4
F20	62.7	14.3	3.0	20.0	2.5±0.4	68.3±4.2	0.015±0.002	4.3±2.1

The interfacial adhesion between the nanoparticles and the polymer was assessed by studying the stress–strain patters of films. **Figure 1** shows the stress-strain curve of films representative for all studied formulations.

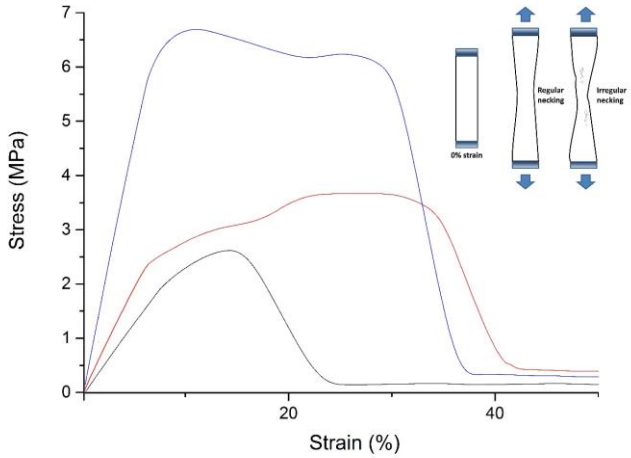

Figure 1. The stress-strain curve of the nanocomposite films representative of all formulations: F0 (black line), F3 (blue line) and F20 (red line). In the insert a schematic representation of films appearance during the tensile test. At nanofiller contents of 3 and 5% w/w, necking occurred after the maximum stress value.

With a further addition of PVAc nanoparticles, the necking onset was modified because PVAc nanoparticles segregated preventing the possibility to carry homogeneously the load.

All films exhibited a linear region at low strain, independently of the composition which is associated to the reversible formation. The higher the slope, the stiffer the material.
Increasing the strain, the behavior shifted from elastic to plastic, the curve lost linearity and the deformation became irreversible, until the maximum force (tensile strength, TS) was reached. Then, the force progressively decrease until the breaking of the film. This behavior was typical of films F0 and F1, meanwhile increasing the nanofiller content in the range 3-5% w/w (films F3 and F5), some remarkable changes can be detected after the TS of the stress-strain curve. Indeed, not only the stress required to deform MDX films significantly increased, but also the maximum value was followed by a pronounced plateau at a lower value which was attributed to necking. With a further addition of PVAc nanoparticles (films F10 and F20), the film behavior appeared to be further modified. Indeed, the film homogenously stretched at low strain before the second yield point. Afterwards, an increase in stress was observed followed by a plateau.
This modification in the onset of necking might be attributed to differences in interfacial strength and degree of dispersion due to the very high specific surface area provided by nanoparticle (Wetzel, Haupert, & Zhang, 2003). Hence, it can be assumed that well distributed PVAc nanoparticles with an adequate interfacial bonding between filler and matrix allows the effective transfer of stress through a shear mechanism from the matrix to the particles that can efficiently carry the load and enhance the strength of the composite (films F3 and F5). At highest filler content (films F10 and F20), PVAc nanoparticles segregated within the matrix and the film consisted on a system which does not carry homogeneously the load.
These trends are in agreement with the quantitative evaluation of the stress-strain curves (**Table 1**). The control film F0 exhibited a low tensile strength of about 1.8 MPa. Low nanofiller contents resulted in the maximum increase of the film stiffness suggesting that PVAc acts as an effective reinforcing agent at the concentration of 3 and 5 % w/w. Similar results were observed for the toughness, expressed as the tensile energy to break, and the tensile strength. With a further addition of nanofiller, both the mechanical properties progressively decreased, suggesting a weak load transfer from the matrix to nanofiller and/or the failure of the nanofiller included in matrix. As mentioned above, this features may due to the volume fraction of PVAc which is related to the formation of aggregates (Bréchet et al., 2001; Liu, Zhong, Chang, Li, & Wu, 2010; Wang & Zhang, 2008).
It is worthy to notice the progressive reduction of the elastic modulus at the highest nanofiller concentration is concomitant to a significant increase of the elongations at break with respect to the other formulations ($p<0.05$, **Table 1**). A possible reason lies in the fact that the formation of aggregates made

some hydroxyl groups along MDX chains available again for the interaction with water molecules, resulting in an enhanced plasticizing effect. This effect is very similar to that obtained by loading of 10% quercetin nanocrystals which reduced the elastic modulus and increased the elongation at break of the loaded films (Lai et al., 2015).

3.2. Molecular characterization

To better understand the mechanism causing the mechanical reinforcing in films, mixtures of spray-dried MDX and PVAc in different ratios were characterized at molecular level using a combination of DSC and ATR-FTIR spectroscopy.

DSC data revealed that during the first heating ramp the PVAc glass transition (T_g) was measured in the temperature range 25-41 °C, with an inflection at about 34 °C. This value overlapped the event in the subsequent reheating ramp. Another endothermic peak appears at the temperature higher than 180 °C, probably associated to the thermal decomposition of sodium lauryl sulfate, which is used to stabilize the commercial PVAc used in this study. DSC measurement of the pure MDX showed the T_g at 102.6±2.0 °C. Both distinct events were observed in all composition range, without significant shift in T_g comparing to the single components, suggesting that no chemical reaction or extensive physical interaction between the polymeric components occurred (**Figure 2**). In other word, a very poor miscibility between PVAc and MDX can be assumed.

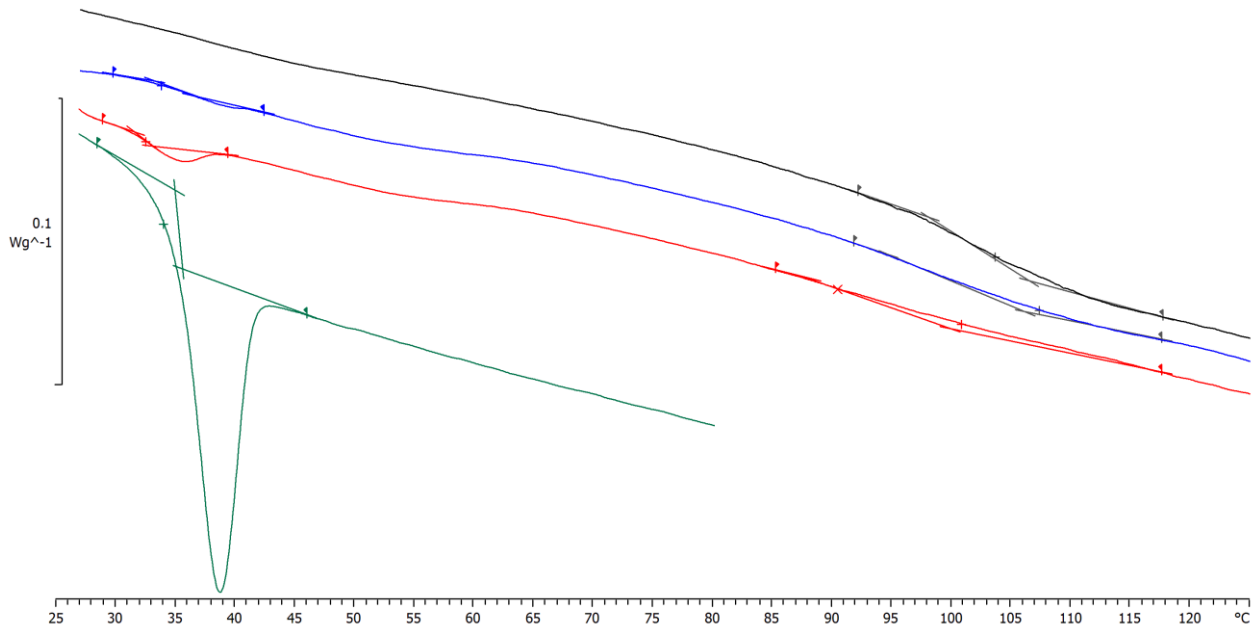

Figure 2. Thermal data of dried PVAc (green line) MDX (black line) and the binary mixtures containing 5% (blue line) and 20% PVAc (red line).

The mixtures were also subjected to an ATR-FTIR analysis in order to provide some insights into the conformational features. The spectra of dried MDX and PVAc were taken as reference samples to identify the diagnostic bands (**Figure 3**).

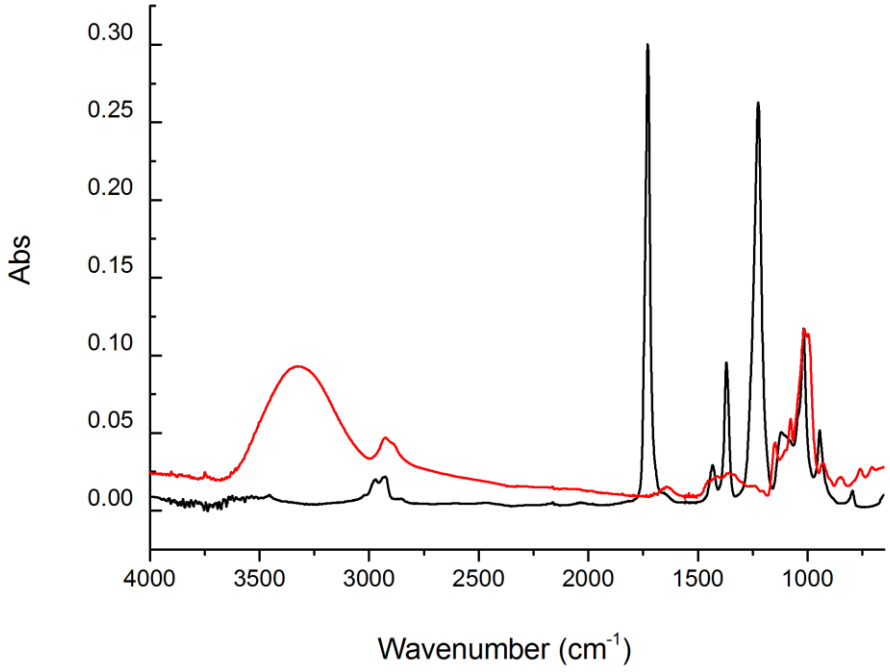

Figure 3. ATR-FTIR spectra of spray-dried MDX (red line) and PVAc dried in oven until constant weight (black line).

In particular, the characteristic absorption peaks of PVAc appeared at about 1729 and 1225 cm^{-1} corresponding to the C=O and C-O stretching vibrations, respectively (Wei et al., 2009). The band at 2929 cm^{-1} was attributed to the C-H stretching vibrations band of methyl group.

As far as MDX is concerned, the principal contributions for carbohydrate polymers are generally in the 1300-860 cm^{-1} region. These vibrations were attributed to C-C and C-O stretching, as well as to COH bending (De Giacomo, Cesàro, & Quaroni, 2008). In particular, the band recorded at about 1022 cm^{-1} or lower wavenumbers confirmed that MDX used in the current work is completely amorphous (Van Soest, Tournois, De Wit, & Vliegenthart, 1995). MDX presents also a broad peak centered at 3309 cm^{-1} which originated from the fundamental stretching vibration of the –OH group. Hydroxyl groups rarely exist in isolation because they are usually involved in intra- and inter-molecular hydrogen bonding with other hydroxyl groups.The broad features of this peak are due to the wide range of hydrogen bond lengths and orientations, which exists in the amorphous carbohydrate system. Therefore, its position reflects the

average hydrogen bond strength in a system (Bellamy, 1975). Finally, the short band in the range of 2908-2930 cm^{-1} arise mostly from the C-H deformation vibrations stretching.

In the entire composition range of the MDX/PVAc blends, the main bands of both components were detectable and the minor variations in wavelength and/or peak intensity were attributed to a simple overlapping of the contributes of the two compounds. These data confirming the lack of interaction between MDX and PVAc verified by DSC .

Moving to ODFs in which glycerin and Span® 80 were also added, some relevant modifications in the 1800-1550 cm^{-1} region were noted (**Figure 4**). Firstly, the C=O stretching vibration of PVAc shifted from 1729 cm^{-1} to about 1710 cm^{-1} independently of film composition; secondly, this band became predominant in the formulation containing at least the 10 % w/w PVAc. Finally, the intensity of the C=O stretching vibration band was not linearly related to the nanofiller content.

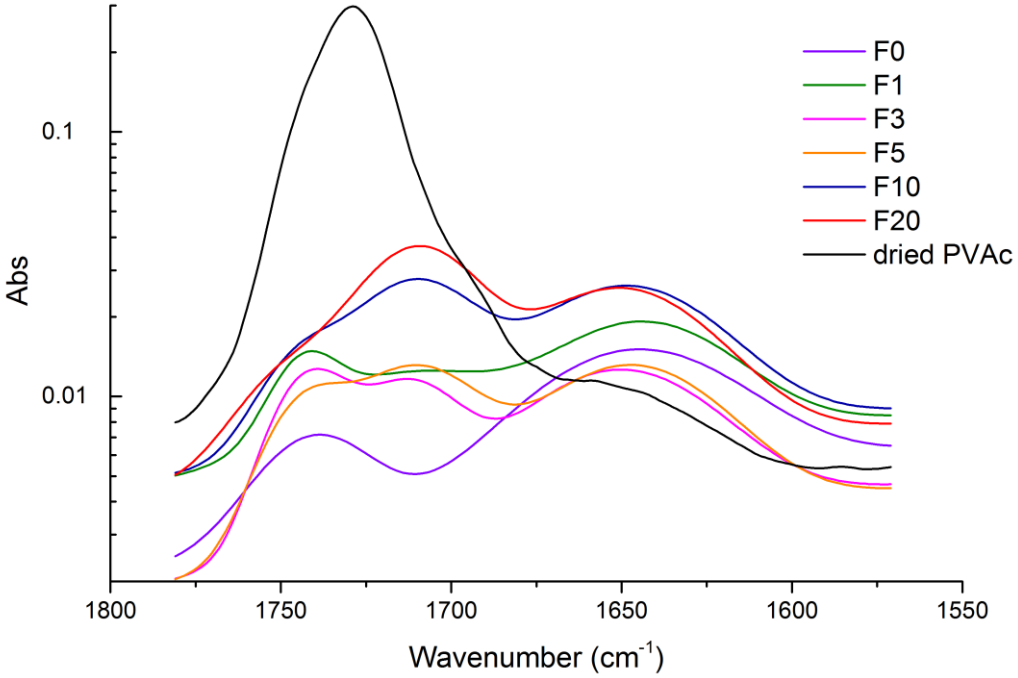

Figure 4. Focus on the 1800-1550 cm^{-1} region of the ATR-FTIR spectra of ODFs containing different concentrations of PVAc and the dried PVAc.

This significant modification in the 1800-1550 cm^{-1} region was concomitant to a slight modification of the band deriving by stretching vibration of hydroxyls at about 3300 cm^{-1}. In this case, the comparison of the spectra recorded on the films and the corresponding binary blends evidenced a reduction in wavenumber and in FWHM (**Table 2**).

All together, these results suggested that MDX in reinforced ODFs is involved in a different type of hydrogen bonds probably mediated by the presence of the plasticizers. The extent of interaction growth according to the PVAc content. As noticed by the shift and depression of the C=O stretching band of PVAc, this interaction may be responsible of the nanoparticles aggregation hypothesized on the tensile data. In other words, at nanofiller content more than 10% the plasticizers resulted insufficient to guarantee a homogeneous dispersion of PVAc that segregated causing the inhomogeneous transfer of the load within the film and, therefore, affecting the film tensile properties.

Table 2 – Full width at half maximum (FWHM) and wavenumber of –OH stretching vibration in binary blends and ODFs.

PVAc content (%)	ODFs		Binary blends	
	Wavenumber (cm^{-1})	FWHM	Wavenumber (cm^{-1})	FWHM
0	3309	332	3335	349
1	3319	348	3334	355
3	3318	342	3336	345
5	3324	343	3335	350
10	3325	346	3335	349
20	3325	339	3336	344

In conclusion, the reinforcement of ODFs by using a nanofiller was successfully obtained by incorporating the commercially available dispersion of PVAc in the 3 to 5 % range.

References:

Bellamy, L. J. (1975). The infra-red spectra of complex molecules (3rd ed.) Chapman and Hall, London.

Borges, A. F., Silva, C., Coelho, J. F .J. & Simões, S. (2015). Oral films: current status and future perspectives I — galenical development and quality attributes. *Journal of Controlled Release, 206*, 1–19.

Bréchet, Y., Cavaillé, J. Y. Y., Chabert, E., Chazeau, L., Dendievel, R., Flandin, L. & Gauthier, C. (2001). Polymer based nanocomposites: effect of filler-filler and filler-matrix interactions. *Advanced Engineering Materials, 3* (8), 571-577.

Chen, B. & Evans, G. J. R. (2005). Thermoplastic starch–clay nanocomposites and their characteristics. *Carbohydrate Polymers, 61*, 455-463.

Cilurzo, F., Cupone, I. E., Minghetti, P., Selmin, F. & Montanari, L. (2008). Fast dissolving films made of maltodextrins. *European Journal of Pharmaceutics and Biopharmaceutics, 70,* 895–900.

Cilurzo, F., Cupone, I. E., Minghetti, P., Buratti, S., Selmin, F., Gennari, C. G. M., Montanari, L. (2010). Nicotine fast dissolving films made of maltodextrins: a feasibility study. *AAPS PharmSciTech., 11* (4), 1511-1517.

Cilurzo, F., Cupone, I. E., Minghetti, P., Buratti, S., Gennari, C. G. M. & Montanari, L. (2011). Diclofenac fast-dissolving film: suppression of bitterness by a taste-sensing system. *Drug Development and Industrial Pharmacy, 37*, 252–259.

De Carvalho, A. J. F., Curvelo, A. A. S. & Agnelli, J. A. M. (2001). A first insight on composites of thermoplastic starch and kaolin. *Carbohydrate Polymers, 45*, 189-194.

De Giacomo, O., Cesàro, A. & Quaroni, L. (2008). Synchrotron based FTIR spectromicroscopy of biopolymer blends undergoing phase separation. *Food Biophysics, 3*, 77-86.

Dixit, R.P., Puthli, S.P. (2009). Oral strip technology: overview and future potential. *Journal of Controlled Release, 139*, 94–107.

European Directorate for the Quality of Medicines (EDQM), 2012. Oromucosal preparation. European Pharmacopoeia Commission in European Pharmacopoeia, 7.4 Edition. EDQM, Strasburg, France.

Fortunati, E., Puglia, D., Kenny, J. M., Haque, M. M., Pracella, M. (2013). Effect of ethylene-co-vinyl acetate-glycidylmethacrylate and cellulose microfibers on the thermal, rheological and biodegradation properties of poly(lactic acid) based systems. *Polymer Degradation and Stability, 98*, 2742-2751.

Kolter, K., Dashevsky, A., Irfan, M. & Bodmeier, R. (2013). Polyvinyl acetate-based film coatings. *International Journal of Pharmaceutics, 457*, 470–479.

Lai, F., Franceschini, I., Corrias, F., Sala, M. C., Cilurzo, F., Sinico, C. & Pini, E. (2015). Maltodextrin fast dissolving films for quercetin nanocrystal delivery. A feasibility study. *Carbohydrate Polymers, 121*, 217-223.

Le Bolay, N. & Molina-Boisseau, S. (2014). Production of PVAc-starch composite materials by co-grinding – influence of the amylopectine to amylose ration on the properties. *Powder Technology, 255*, 36-43.

Le Bolay, N., Lamure, A., Gallego Leis, N. & Suhani, A. (2012). How to combine a hydrophobic matrix and a hydrophilic filler without adding a compatibilizer – co-grinding enhances use properties of renewable PLA-starch composite. *Chemical Engineering Process*, *56*, 1-9.

Liu, D., Zhong, T., Chang, P. R., Li, K. & Wu, Q. (2010). Starch composites reinforced by bamboo cellulosic crystals. *Bioresource Technology, 101*, 2529–2536.

Park, H. W., Lee, W. K., Park, C. Y., Cho, W. J. & Ha, C. S. (2003). Environmentally friendly polymer hybrids - Part I mechanical, thermal, and barrier properties of thermoplastic starch/clay nanocomposites. *Journal of Materials Science*, *38*, 909–915.

Petersson, L. & Oksman, K. (2006). Biopolymer based nanocomposites: Comparing layered silicates and microcrystalline cellulose as nanoreinforcement. *Composites Science and Technology, 66*, 2187–2196.

Selmin, F., Franceschini, I., Cupone, I. E., Minghetti, P., Cilurzo, F. (2015). Aminoacids as non-traditional plasticizers of maltodextrins fast-dissolving films. *Carbohydrate Polymers, 115*, 613-616.

Van Soest, J. J. G., Tournois, H., De Wit, D. & Vliegenthart, J.G., (1995). Short-range structure in (partially) crystalline potato starch determined with attenuated total reflectance Fourier-transform IR spectroscopy. *Carbohydrate Polymers, 279*, 201-214.

Wang, Y. & Zhang, L. (2008). High-strength waterborne polyurethane reinforced with waxy maize starch nanocrystals. *Journal of Nanoscience and Nanotechnology*, *8*, 5831–5838.

Wei, H., Li-Fang, F., Bai, X., Chin-Lei, X., Qing, D., Yong-Zhen, C. & De-Yang, C. (2009). An investigation into the characteristics of chitosan/Kollicoat SR30D free films for colonic drug delivery. *European Journal of Pharmaceutics and Biopharmaceutics, 72*, 266-274.

Wetzel, B., Haupert, F. & Zhang, M. Q. (2003). Epoxy nanocomposites with high mechanical and tribological performance. *Composite Science Technology, 63*, 2055-2067.

Wilhelm, H. M., Sierakowski, M. R., Souza, G. P. & Wypych, F. (2003). Starch films reinforced with mineral clay. *Carbohydrate Polymers, 52*, 101–110.

Figure 1

Click here to download high resolution image

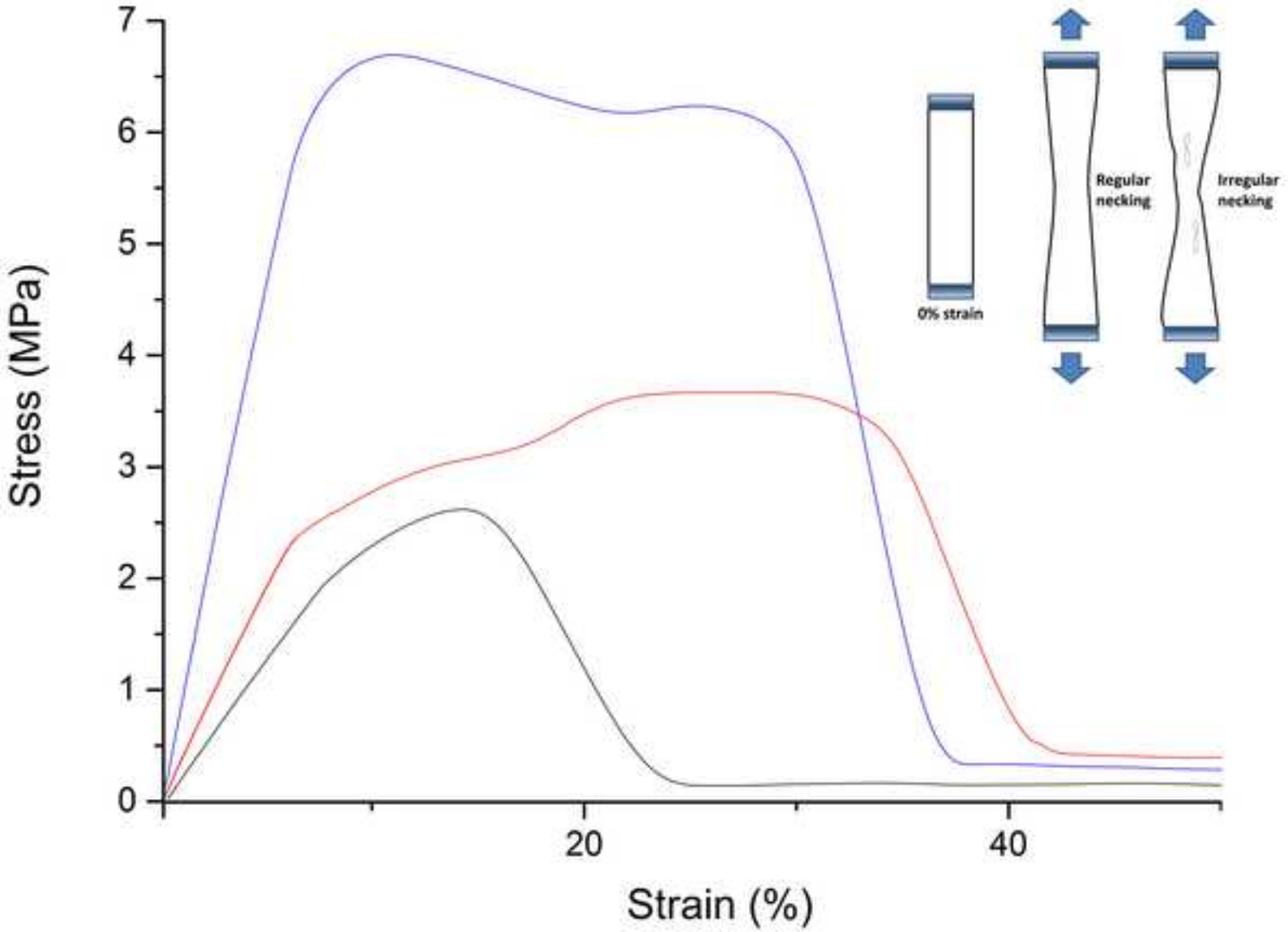

Figure 2

Click here to download high resolution image

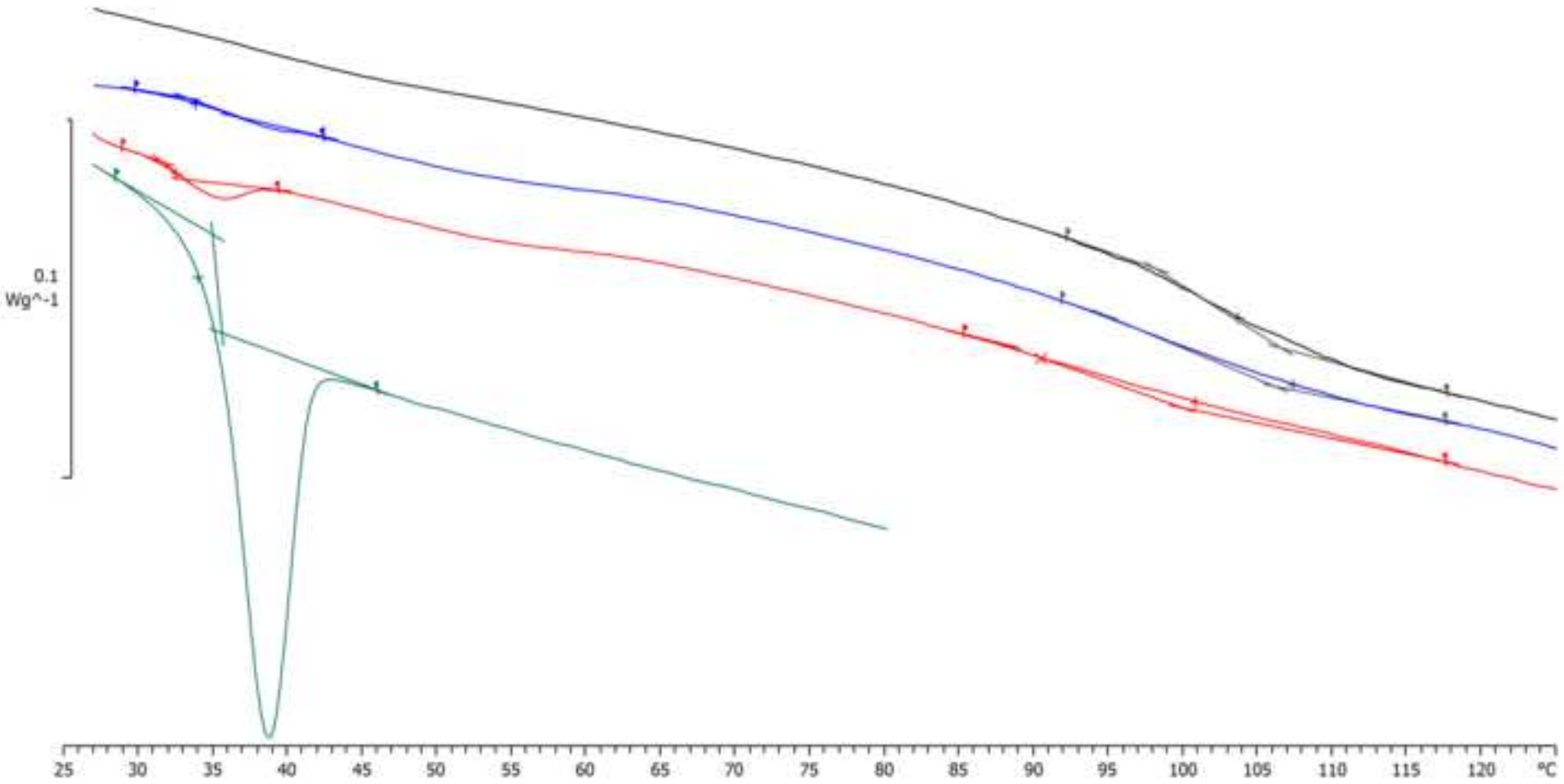

Figure 3

Click here to download high resolution image

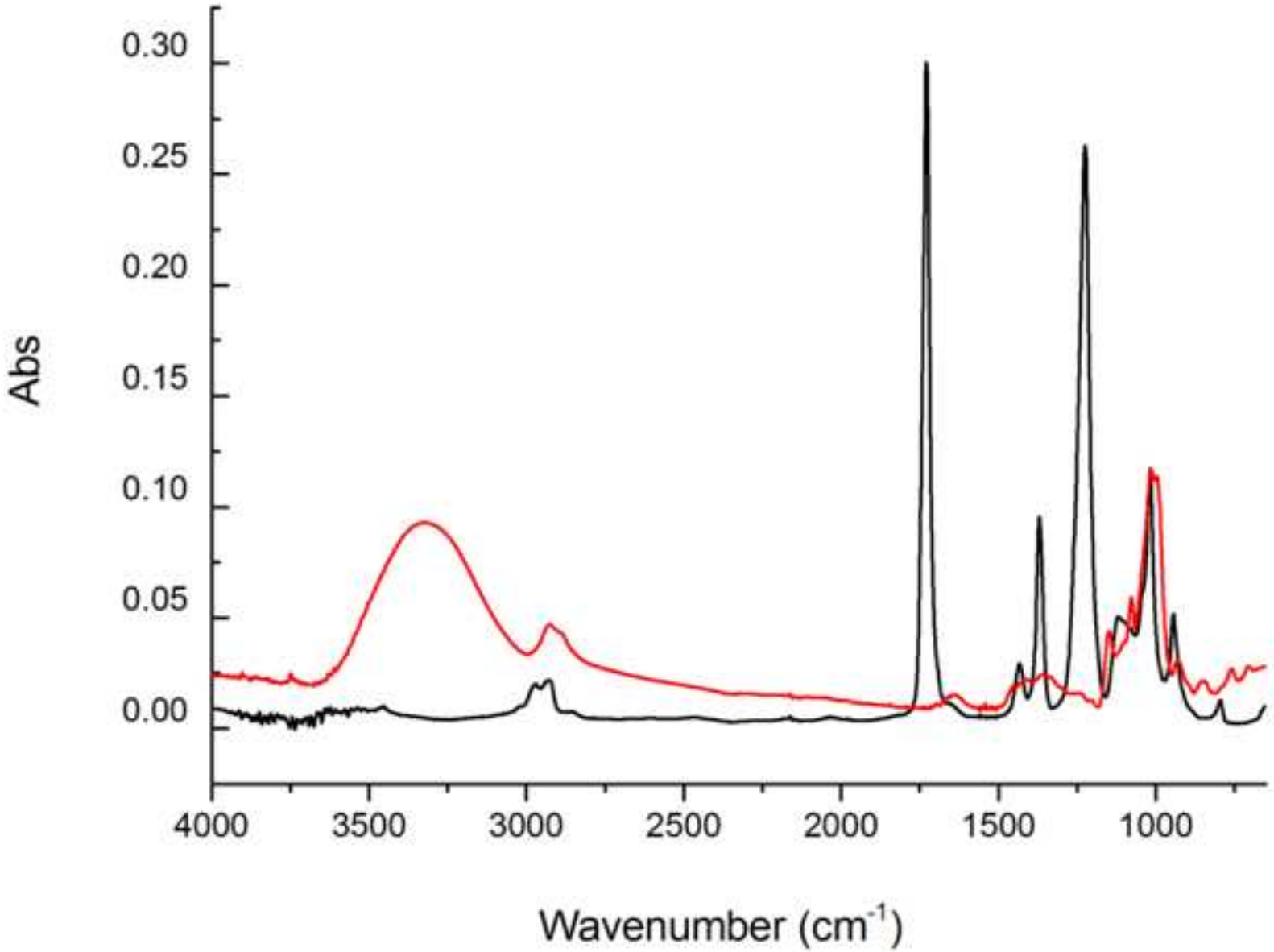

Figure 4

Click here to download high resolution image